# Spatial and Temporal Control of Nonmuscle Myosin Localization: Identification of a Domain That Is Necessary for Myosin Filament Disassembly In Vivo

Thomas T. Egelhoff, Susan S. Brown,* and James A. Spudich

Departments of Cell and Developmental Biology, Stanford University School of Medicine, Stanford, California

*Abstract.* Myosin null mutants of *Dictyostelium* are defective for cytokinesis, multicellular development, and capping of surface proteins. We have used these cells as transformation recipients for an altered myosin heavy chain gene that encodes a protein bearing a carboxy-terminal 34-kD truncation. This truncation eliminates threonine phosphorylation sites previously shown to control filament assembly in vitro. Despite restoration of growth in suspension, development, and ability to cap cell surface proteins, these ΔC34-truncated myosin transformants display severe cytoskeletal abnormalities, including excessive localization of the truncated myosin to the cortical cytoskeleton, impaired cell shape dynamics, and a temporal defect in myosin dissociation from beneath capped surface proteins. These data demonstrate that the carboxy-terminal domain of myosin plays a critical role in regulating the disassembly of the protein from contractile structures in vivo.

T HE production of myosin-deficient mutants in *Dictyostelium* by generation of antisense RNA (Knecht and Loomis, 1987) and by homologous recombination (De Lozanne and Spudich, 1987; Manstein et al., 1989) has provided direct genetic evidence that myosin is essential for cytokinesis and for completion of *Dictyostelium*'s multicellular developmental program. Studies with these mutants have also demonstrated that myosin is involved in movements of cortically linked membrane proteins, as evidenced by the inability of myosin-deficient cells to cap con A cross-linked surface proteins (Pasternak and Spudich, 1989; Fukui et al., 1990).

Although a reasonably clear picture of the roles of nonmuscle myosin is beginning to emerge, the mechanisms controlling assembly and localization of myosin structures in vivo are not well understood. Relocalization of myosin in response to cellular signals occurs during cytokinesis, chemotaxis, and capping of surface receptors (Kitanishi-Yumura and Fukui, 1989; Yumura et al., 1984; Carboni and Condeelis, 1985; Schreiner et al., 1977). In all of these examples, myosin-containing contractile structures must be correctly localized, assembled, activated for contraction, and eventually disassembled. The feasibility of introducing altered myosin genes into myosin null cells now makes it possible to identify domains of the protein that are critical for these in vivo activities.

Several lines of evidence suggest that the myosin domains that drive assembly and regulate assembly lie within the α-helical coiled-coil tail. Muscle myosin can be proteolyti-

cally fragmented into heavy meromyosin (HMM)[1] and light meromyosin (LMM), where the HMM fragment contains the globular head and the amino-terminal third of the tail, and the LMM fragment contains the carboxy-terminal two thirds of the tail. Numerous studies have demonstrated that the domains that drive filament assembly lie within the LMM portion of the molecule (Harrington and Rodgers, 1984). These observations have been confirmed and extended with *Dictyostelium* myosin HMM and LMM fragments. When *Dictyostelium* HMM is produced in vivo in cells devoid of normal myosin, a diffuse distribution is observed by immunomicroscopy, indicating that the HMM molecule cannot assemble into thick filaments, and is not capable of subcellular localization (Fukui et al., 1990). Conversely, an assembly domain has been identified within the LMM region by an mAb study (Pagh et al., 1984) and by recombinant genetics (O'Halloran et al., 1990). A genetically engineered subfragment located from 34 to 68 kD from the carboxy terminus of the tail (N34; see Fig. 1) can assemble into LMM-type paracrystals. The salt dependence of this assembly is similar to that of intact myosin. Other LMM subfragments are not capable of assembling, suggesting that this domain may be the primary region driving assembly of the intact protein.

The last 34 kD of the tail (C34; see Fig. 1) may regulate assembly. Many cytoplasmic myosins are phosphorylated by heavy chain kinases, with consequent changes in their as-

---

1. *Abbreviations used in this paper*: HMM, heavy meromyosin; LMM, light meromyosin.

**Head** (93 kD)                      **Tail** (150 kD)
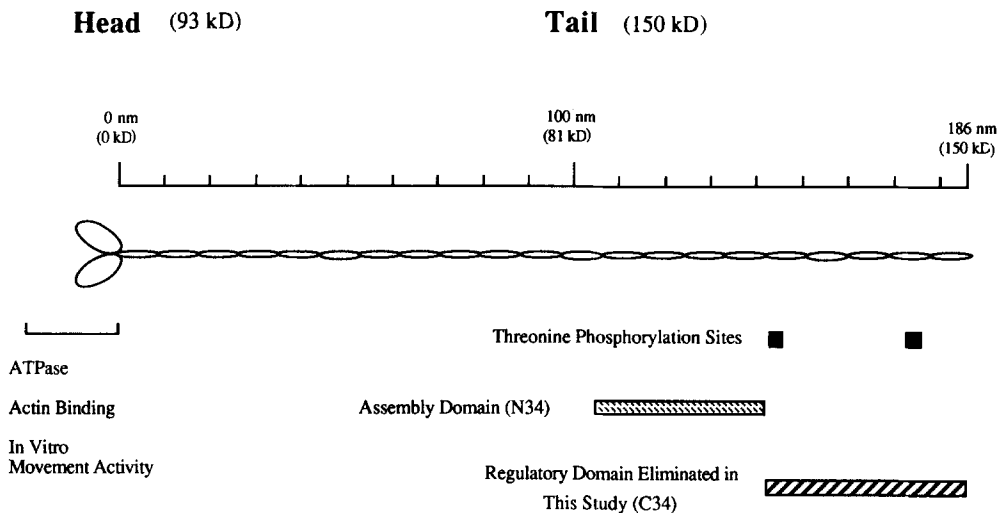


*Figure 1.* Schematic diagram of *Dictyostelium* myosin illustrating the positions of previously identified threonine phosphorylation and assembly domains as well as the position of the C34 domain that is the focus of this study. Scale indicates distance from the head–tail junction; divisions represent 10 nm or 8.1 kD.

sembly properties (Collins et al., 1982; Ogihara et al., 1983; Cote and McCrea, 1987; Kuczmarski et al., 1987; Ravid and Spudich, 1989). In *Dictyostelium*, phosphorylation of specific threonines near the carboxy terminus of myosin by a purified myosin heavy chain kinase inhibits assembly in vitro at physiological salt levels. Three phosphorylatable residues have been identified in the C34 domain by an mAb study (Pagh et al., 1984) and by peptide sequencing (Vaillancourt et al., 1988; see Fig. 1). These three residues have been independently identified as phosphorylation targets by expression in *E. coli* of myosin tail fragments in which individual threonine residues were converted to alanine or serine residues and tested for ability to be phosphorylated by *Dictyostelium* kinase preparations (Luck-Vielmetter et al., 1990). In vivo, myosin relocalization in response to cAMP stimulation has been correlated with transient heavy chain phosphorylation, suggesting that heavy chain phosphorylation may play a role in the relocalization process (Berlot et al., 1987; Nachmias et al., 1989).

To identify the in vivo roles of this carboxy-terminal 34 kD of the myosin tail, we have transformed myosin null cells with an extrachromosomal vector expressing either the full-length myosin gene or a myosin gene bearing a truncation that eliminates the terminal 34 kD of the tail. This ΔC34 truncation removes the sites known to undergo threonine phosphorylation, but leaves intact the assembly domain that has been identified by *E. coli* expression studies (Fig. 1). The results reported here indicate that the carboxy-terminal domain of *Dictyostelium* myosin is not necessary for in vivo contractile activity, but that it is critical for regulating the extent of myosin assembly in vivo and for proper control of cortical localization.

## Materials and Methods

### Plasmid Constructs

The plasmid pSB2 was constructed using the extrachromosomal hygromycin-resistance vector pDE109 (Egelhoff et al., 1989). pDE109 was restricted with Bam HI and Kpn I, and treated with Klenow enzyme to create blunt ends. A 7.7-kb Sph I–Mlu I fragment from pDE105 (Egelhoff et al., 1990) that contains the actin 15 promoter and the first eight codons of the actin 15 coding region fused to the third codon of the myosin heavy chain

gene was isolated, treated with Klenow enzyme to create blunt ends, and ligated into the pDE109 described above. The resulting plasmid pSB2 has the myosin and hygromycin resistance genes in a convergent orientation, with both genes sharing the same actin 15 terminator sequence.

The plasmid pSB3 was constructed by replacing a 2.6-kb Kpn I–Spe I fragment of pSB2 with a 1.4-kb Kpn I–Spe I fragment from pMyΔC34 (O'Halloran and Spudich, 1990). This substitution leaves the 5' end of the myosin construct intact, but introduces a truncation after amino acid 1,819 of the myosin heavy chain (two extra amino acids, arginine and serine, are introduced after the aspartate residue at position 1,819, directly followed by a stop codon).

### Manipulations of Dictyostelium Cells

Cell lines used in these studies include the Ax2 strain of *Dictyostelium discoideum* and a myosin null mutant, HS2206, that was generated from the Ax2 line by gene targeting in the manner described by Manstein et al. (1989) for the cell lines mhcA⁻/A5-2 and mhcA⁻/A5-3. These cell lines have been renamed HS2202 and HS2203, respectively, using rules outlined by Demerec et al., 1966.

Cells were grown adhering to Falcon tissue culture plates containing 10 ml of HL5 medium (Sussman, 1987). Growth curves in suspension culture were obtained by resuspending cells from plates into HL5 medium (omitting hygromycin). 10-ml suspensions of 5 × 10⁴ cells/ml were placed in 50-ml flasks on a rotary platform, and cell counts were made daily using a hemocytometer.

For video microscopy, cells were resuspended from plates and placed as hanging drops in a chamber formed by a greased rubber o-ring between a slide and coverslip. Samples were filmed for no more than 1-2 h before being replaced by fresh material. Time lapse photography was carried out using video-enhanced differential interference contrast microscopy, and images were recorded on a Panasonic optical memory laser disc.

Transformations were done as described previously (Egelhoff et al., 1989). Briefly, 10⁷ myosin null cells were electroporated with 5 μg of pDE109, pSB2, or pSB3, plated overnight in HL5, then grown in the presence of hygromycin in 96-well microtiter plates. Cells were usually diluted tenfold, and 60 μl were added per well of the microtiter plate in order to obtain approximately ten positive clones per plate and thus ensure clonality. Transformants were grown in 20 μg/ml hygromycin during initial characterization; at later stages growth in suspension was used to select for maintenance of the myosin expression plasmids.

### Electrophoretic Methods

Southern blot analysis was performed as described by Egelhoff et al. (1989). Genomic DNA samples were isolated ∼4-5 wk after the transformation of the plasmids into the myosin null cell line. Electrophoresis conditions were adjusted to optimize separation of the supercoiled and nicked closed circular plasmid DNA from the sheared chromosomal DNA. Samples were electrophoresed in a 0.6% agarose gel in TAE buffer (Maniatis et al., 1982) in the absence of ethidium bromide at 80 V (4.5 V/cm gel bed) for 16 h. The
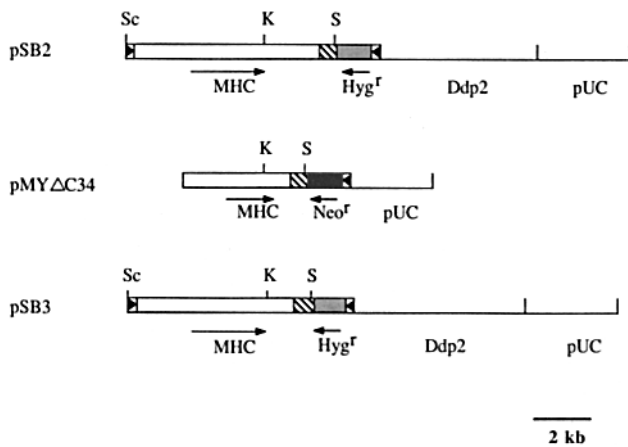
        

*Figure 2.* Plasmid maps. Fill patterns: (*open boxes*) coding sequence of the myosin heavy chain (*MHC*) gene; (*boxed arrowheads*) actin 15 promoter; (*diagonal hatch boxes*) actin 15 terminator; (*black box*) neomycin resistance gene; (*stippled boxes*) hygromycin resistance gene. The positions of sequences from Ddp2 (an endogenous *Dictyostelium* plasmid) and pUC are also indicated. pSB3 was constructed by replacing the indicated Kpn I (*K*)–Spe I (*S*) fragment of pSB2 with an analogous fragment from pMyΔC34 (O'Halloran and Spudich, 1990) in which the myosin gene is truncated at amino acid 1,819 of the MHC coding region.

Southern filter was probed with a 3.1-kb Cla I restriction fragment of the myosin gene corresponding to nucleotides 1,540–4,624 of the coding region.

Western blot analysis was performed on whole cell lysates, which were prepared as described by De Lozanne and Spudich (1987). Protein was determined by the method of Peterson (1977), and lysates were electrophoresed on an 8% SDS-polyacrylamide gel (Laemmli, 1970). Western transfer was carried out as described by Towbin et al. (1979). The filter in Fig. 3 was probed with a rabbit polyclonal antibody directed against *Dictyostelium* myosin (Berlot et al., 1985), and the filter in Fig. 7 was probed with the antimyosin monoclonal My4 (Peltz et al., 1985); these primary incubations were followed by an HRP-coupled secondary antibody, as described previously (De Lozanne and Spudich, 1987).

For quantitation of myosin expression levels, late-log phase cell cultures in HL5 were harvested, washed twice in 50 mM Tris pH 7.5, then suspended in lysis buffer consisting of 50 mM Tris, pH 8.0, 5 mM EDTA, 5 mM EGTA, 1% SDS, 10 μg/ml RNase A, 0.1 mg/ml PMSF, 10 μg/ml pepstatin, 1 μg/ml leupeptin, and 50 μg/ml L-l-chloro-3-[4-tosylamido]-7-amino-2-heptanone-HCl (TLCK). These samples were immediately heated to 100°C for 10 min, then stored at −20°C. Equal amounts of total protein from each extract (determined with the Bio-Rad dye-binding assay) were subjected to SDS-PAGE. These gels were stained with Coomassie blue, destained, then scanned with an LKB laser densitometer to determine the amount of myosin in each gel lane. Scans of the entire lanes (excluding the region of the myosin band) were integrated and used to normalize any differences in loading between lanes. Two adjustments were performed on the initial scans of the myosin bands. First, the values for all truncated myosin scans were divided by 0.86, which corrects for the fact that the ΔC34-truncated myosin is 14% shorter than full-length myosin. Second, two bands that comigrate with full-length myosin are revealed in gel lanes containing only the truncated myosin (these are also seen in cell extracts devoid of any myosin). Coomassie staining due to these two bands could be determined in the truncated myosin extracts since the truncated protein migrates at a lower position on the gels. The staining intensity of these bands was subtracted from the initial scan values for the full-length myosin and the correct values were expressed as a percent of the signal in the Ax2 wild type extract loaded on the same gel. Duplicate gels were run and the results were averaged and used to determine standard deviations.

### Capping and Immunomicroscopy

For the time course of capping presented in Fig. 9, cells in a small drop of HL5 were attached to glass coverslips for 5 min, rinsed into starvation buffer (20 mM morpholinoethanesulfonic acid (MES), pH 6.8, 0.2 mM

CaCl₂, 2 mM MgSO₄,), then incubated in 30 μg/ml tetramethylrhodamine-conjugated con A (TRITC-con A; Sigma Chemical Co., St. Louis, MO) in starvation buffer for 1 min. Excess con A was removed by rinsing attached cells briefly in starvation buffer. Cells were fixed at the indicated time points with 2% formalin in starvation buffer for 10 min. Coverslips were rinsed and mounted in glycerol for fluorescence microscopy.

For the experiments colocalizing myosin with caps, cells were treated with con A as described above. After rinsing back into starvation buffer, cells were overlaid with a thin agar sheet until the time of fixation. This agar overlay technique generally improves preservation of small cells such as *Dictyostelium* (Fukui et al., 1987). We found that the application of the agar sheet improved the synchrony of capping, and had no adverse effect on the rate of capping. The agar sheet also improved retention of the cells to the glass coverslip during fixation. At the indicated time points, cells were fixed in 1% formalin in acetone at −10°C for 5 min. Coverslips were rinsed in PBS before proceeding to antibody incubations. Other details of the immunomicroscopy were done as previously described for the agar overlay technique (Fukui et al., 1987), with minor modifications that we have described previously (Egelhoff et al., 1990). Primary and secondary antibody incubations were done in PBS containing 1% BSA at 37°C for 30 min, each followed by three rinses in PBS. A rabbit polyclonal antiserum directed against *Dictyostelium* myosin was used at a 1:300 dilution, followed by fluorescein-conjugated, affinity-purified goat anti-rabbit IgG (Cappell), used at a 1:30 dilution.

### Isolation of Triton-insoluble Cytoskeletons

Triton-insoluble cytoskeletons and Triton-soluble fractions of cells were isolated as described previously (Spudich, 1987), with modifications described below. 1.5 × 10⁶ cells from log phase cultures were washed twice in 10 mM Tris, pH 7.5, 100 mM KCl, then resuspended in 150 μl of 0.1 M MES, pH 6.8, 2.5 mM EGTA, 5 mM MgCl₂, and 0.5 mM ATP at 0°C. An equal volume of the same buffer containing 1% Triton X-100, 0.1 mg/ml PMSF, 10 μg/ml leupeptin, 50 μg/ml TLCK, and 10 μg/ml pepstatin was added, and the suspension vortexed for 5 s at medium setting. The lysed mixture was then centrifuged for 1 min in a microfuge. The Triton-insoluble pellet was dissolved in SDS gel sample buffer and heated to 100°C for 5 min. The Triton-soluble supernatant was precipitated by addition of 700 μl of acetone and incubation on ice (10 min), then pelleted and resuspended in SDS gel sample buffer as above. SDS-PAGE was performed, and the re-
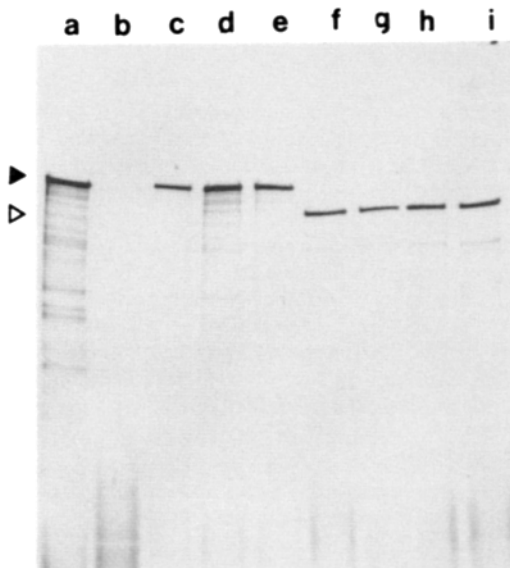


*Figure 3.* Western blot analysis. 5 μg of total protein from different cell lines is loaded in lanes *a–i.* (lane *a*) Ax2; (lane *b*) myosin null cell line HS2206 transformed with the vector alone (pDE109); (lanes *c–e*) HS2206 cells transformed with pSB2 expressing full-length myosin; (lanes *f–i*) HS2206 cells transformed with pSB3 expressing the truncated myosin. The solid arrowhead indicates the position of full length myosin (240 kD), and the open arrowhead indicates the position of the truncated myosin (205 kD).
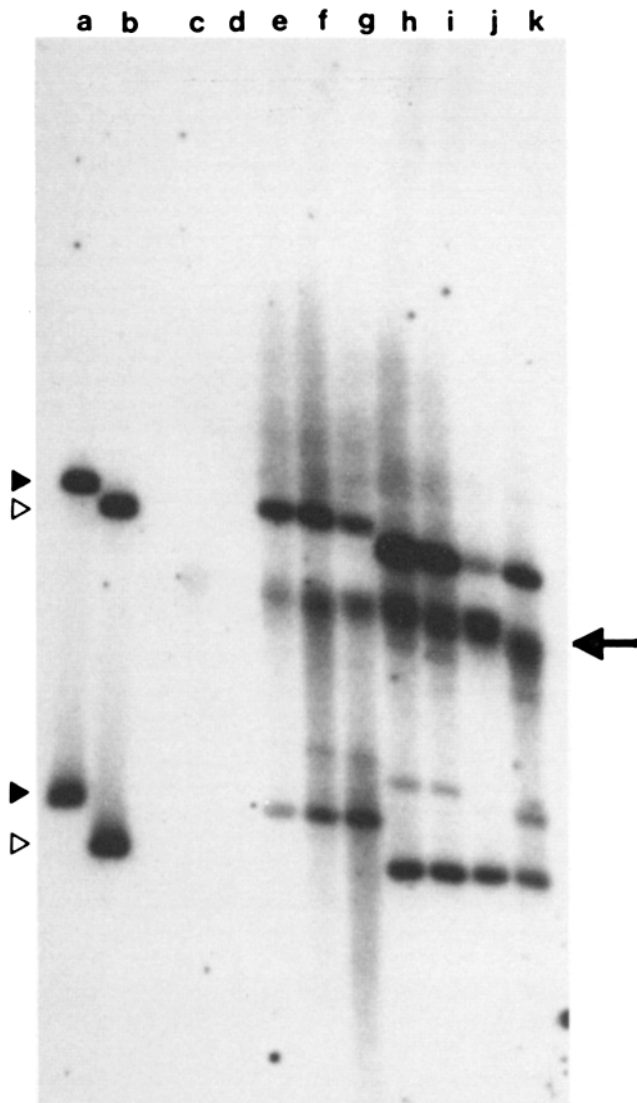
*Figure 4.* Southern blot analysis. Undigested total DNA samples were electrophoresed on an agarose gel to resolve circular and sheared linear DNA. The arrow at the right margin indicates the position of migration of the linear sheared chromosomal DNA. At the left margin, filled arrowheads indicate the position of migration of pSB2 in nicked circular form (*upper*) and supercoiled form (*lower*); the open arrowheads indicate the position of migration of pSB3 in nicked circular form (*upper*) and supercoiled form (*lower*). (lane *a*) Purified pSB2 DNA; (lane *b*) purified pSB3 DNA; (lane *c*) Ax2 wild type DNA; (lane *d*) HS2206 null cell DNA; (lanes *e–g*) DNA from null cells transformed with pSB2; (lanes *h–k*) DNA from null cells transformed with pSB3.

solved proteins were either transferred to nitrocellulose filters for Western blot analysis as described above, or stained with Coomassie blue.

## Results

Transformation of the myosin null cell line HS2206 with the plasmids pSB2 or pSB3 (Fig. 2) resulted in cells that express full-length or truncated myosin, respectively, as seen by Western blot analysis (Fig. 3). The expression level of the original Ax2 cells is shown in lane *a*, and the absence of myosin expression in myosin null cells transformed with vector

alone is shown in lane *b*. Three cell lines with the full-length myosin introduced (lanes *c–e*) all express myosin at levels roughly similar to wild type cells, and four cell lines with the ΔC34-truncated myosin (lanes *f–i*) introduced all expressed the protein at levels somewhat lower than wild type cells. After initial characterization, one full-length and one truncated myosin cell line were chosen for further studies. Densitometer scans of the myosin bands in SDS-polyacrylamide gels of cell extracts of these cell lines revealed that expression in the full-length myosin transformants was 91% ($\pm$18; $n = 6$) of the wild type level, and expression in the ΔC34-truncated myosin transformants was 42% ($\pm$8; $n = 6$) of the wild type level.

Southern blot analysis of these transformants confirmed that pSB2 and pSB3 were present and appear to be maintained extrachromosomally (Fig. 4). DNA isolated from three pSB2 transformants (Fig. 4, lanes *e–g*) demonstrated that much of the plasmid migrates at the position of supercoiled or nicked circular plasmid. Some plasmid also migrates at the position of the sheared chromosomal DNA. A similar pattern is seen for the pSB3 transformants (Fig. 4,
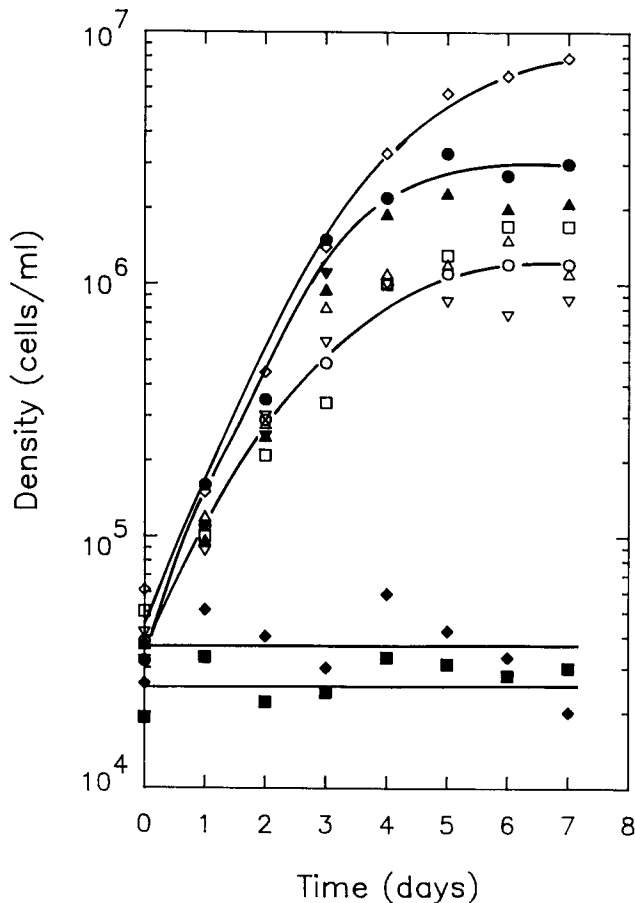


*Figure 5.* Growth curves. On day 0, parallel aliquots of cells growing on plates were placed into suspension culture or prepared for the western blots shown in Fig. 3. Cells are wild type Ax2 (*open diamonds*), HS2206 myosin null cells (*filled diamonds*), three pSB2 transformants of HS2206 (*filled triangles* and *filled circles*), four pSB3 transformants of HS2206 (*open triangles, open circles,* and *open squares*), and HS2206 null cells transformed with vector alone (*filled squares*).
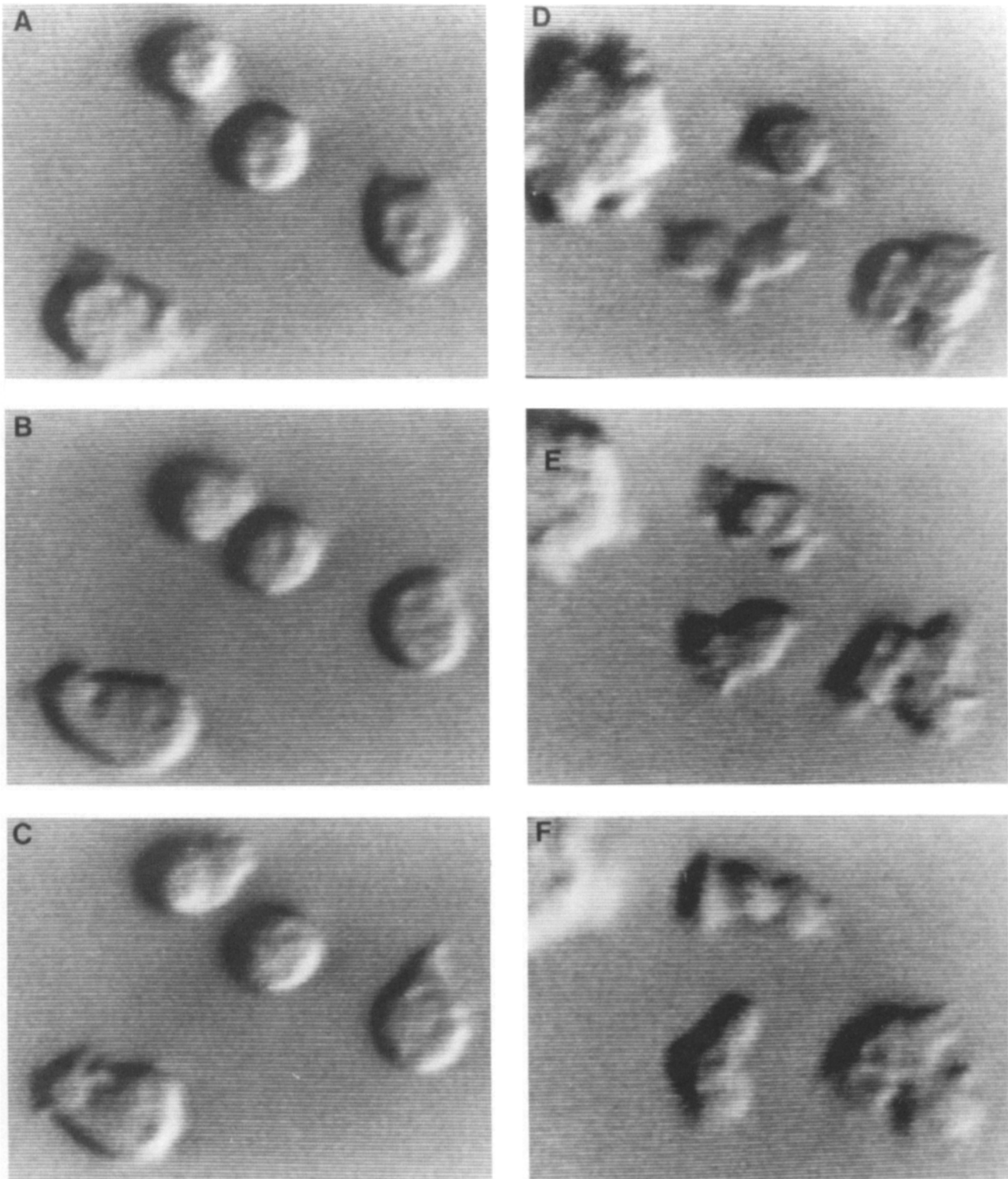
*Figure 6.* Video microscopy of cells in suspension. *A–C* show HS2206 cells transformed with pSB2 at three consecutive 1-min intervals. *D–F* show HS2206 cells transformed with pSB3 at three consecutive 1-min intervals. The stiff, multilobed appearance of the ΔC34-truncated myosin cells is apparent in *D–F.*

lanes *h–k*). The resolution of high molecular weight linear DNA with these electrophoresis conditions is such that the sheared chromosomal DNA often runs at a position similar to size standards in the 20-kb range; we are not certain therefore whether the myosin homology migrating at the position of the chromosomal DNA represents integrated plasmid copies or sheared plasmids that are comigrating with the chromosomal material. It is clear, however, that a substantial portion of the introduced plasmid DNA has remained extrachromosomal.
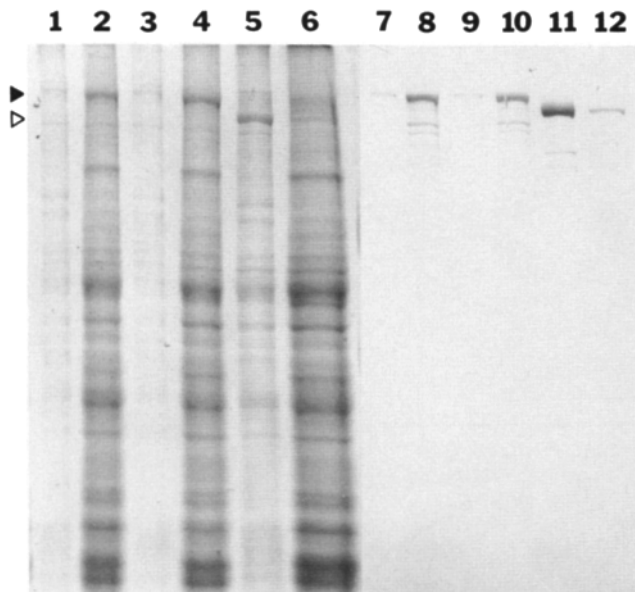
*Figure 7.* SDS–PAGE of Triton-insoluble cytoskeleton fractions and Triton-soluble fractions. Triton-soluble and Triton-insoluble fractions of cell lysates were subjected to SDS–PAGE and stained with Coomassie blue (lanes *1–6*). A duplicate gel was blotted to a nitrocellulose filter and probed with an mAb specific to *Dictyostelium* myosin (lanes *7–12*). Odd-numbered lanes contain Triton-insoluble fractions and even-numbered lanes contain Triton-soluble fractions. (lanes *1, 2, 7,* and *8*) Wild type Ax2 fractions; (lanes *3, 4, 9,* and *10*) full-length myosin transformant fractions; (lanes *5, 6, 11,* and *12*) ΔC34-truncated myosin transformant fractions. The solid arrowhead to left indicates position of wild type and full-length myosin; the open arrowhead indicates the position of the ΔC34-truncated myosin.

To assay competence for cytokinesis, we placed the full-length and ΔC34-truncated myosin transformants in suspension culture and monitored growth. Wild type Ax2 cells grow in suspension with a doubling time of ~8–10 h (Fig. 5, *open diamonds*). Myosin null cells are unable to grow in suspension due to their defect in cytokinesis (Fig. 5, *filled diamonds*); these null cells become large and multinucleated and eventually lyse. In this assay, full-length myosin transformants grew at rates very similar to the Ax2 wild type cells (Fig. 5, *filled circles* and *filled triangles*), and the ΔC34-truncated myosin transformants grew at rates only slightly slower than the wild type Ax2 cells (Fig. 5, *open triangles, squares,* and *circles*).

Video microscopy was performed to examine the behavior of the ΔC34-truncated myosin transformants in suspension. Transformants containing full-length myosin behaved like wild type cells, in that they appeared generally round and actively extended and retracted projections (pseudopodia and filopodia) of the cell surface (Fig. 6, *A–C*). Transformants containing the truncated myosin underwent dramatic rapid deformations from a round shape, often appearing multilobed, with rigid lobes persisting several minutes or longer before being reabsorbed (Fig. 6, *D–F*). Extensions and retractions of pseudopodia and filopodia were not obvious in the truncated myosin cells; the deformations in shape and formation of stiff lobes may represent attempts to form pseudopodia, but these structures are very different in appear-

ance and in dynamics from the pseudopodia of the control cells or wild type cells.

The ΔC34-truncated myosin transformants, while capable of growing in suspension, form multinucleated cells, which indicates abnormalities in the cell division process. In three cases where cell division events were observed in suspension by differential interference contrast microscopy, the cells showed multiple furrows and ultimately divided into an uneven number of daughter cells that varied by as much as two-fold in size from one another. In contrast, several division events observed in the full-length myosin transformants all resulted in two daughter cells of equal size. These observations suggest that the ΔC34-truncated myosin is capable of driving cytokinesis, but does so in an imperfect manner.

We also examined the ability of the transformants to develop. When cells taken from suspension culture were plated on MES starvation plates (Sussman, 1987), both full-length and ΔC34-truncated myosin transformants were able to complete development, forming fruiting bodies and producing spores (data not shown).

As an initial test of the in vivo assembly properties of the truncated myosin we prepared actin-enriched Triton-insoluble cytoskeletons by lysis of cells in the presence of EGTA and Triton X-100 (Spudich, 1987). Comparison of these Triton-insoluble cytoskeletons with the Triton-soluble fractions resolved on SDS-polyacrylamide gels revealed defective myosin localization in the truncated myosin transformants (Fig. 7). Myosin in wild type cells and in the full-length myosin transformants fractionates primarily in the Triton-soluble fraction (Fig. 7, lanes *2, 4, 8,* and *10*), while the majority of the ΔC34-truncated myosin fractionates with the Triton-insoluble cytoskeleton (Fig. 7, lanes *5* and *11*). Densitometric scans of a typical fractionation indicated that 13% of wild type myosin and 13% of the full-length myosin fractionated with the Triton-insoluble cytoskeleton in Ax2 cells and full-length myosin transformants, respectively. In contrast, in the ΔC34-truncated myosin transformants, 80% of the myosin fractionated with the Triton-insoluble cytoskeletons.

Immunomicroscopy was performed to examine myosin distribution. Staining of full-length myosin transformants with an antimyosin antiserum revealed a myosin distribution that was indistinguishable from that of the wild type Ax2 cells. In these cells the myosin is evenly distributed throughout the cortex of the cell as a loose fibrous network (Fig. 8, *A–C*). In contrast, myosin distribution in the truncated myosin transformants is highly abnormal. The majority of these cells contain dense cortical patches of myosin that are not evenly dispersed. These patches vary considerably in size between cells, but usually occupy only a fraction of the cell cortex, with the remainder of the cortex being relatively devoid of myosin staining (Fig. 8, *D–F*). Through-focusing on these cells indicated clearly that these arrays of myosin were in the cortices of the fixed cells and not in the endoplasm. Control staining of these cells with secondary antibody alone resulted in extremely faint diffuse fluorescence. Furthermore, staining of the myosin null cell line HS2206 with the antimyosin antiserum and secondary antibody also resulted in extremely faint diffuse fluorescence, confirming the specificity of the immunostaining (data not shown).

As a further assay of in vivo myosin function, we tested the ability of these cells to cap cell surface glycoproteins in
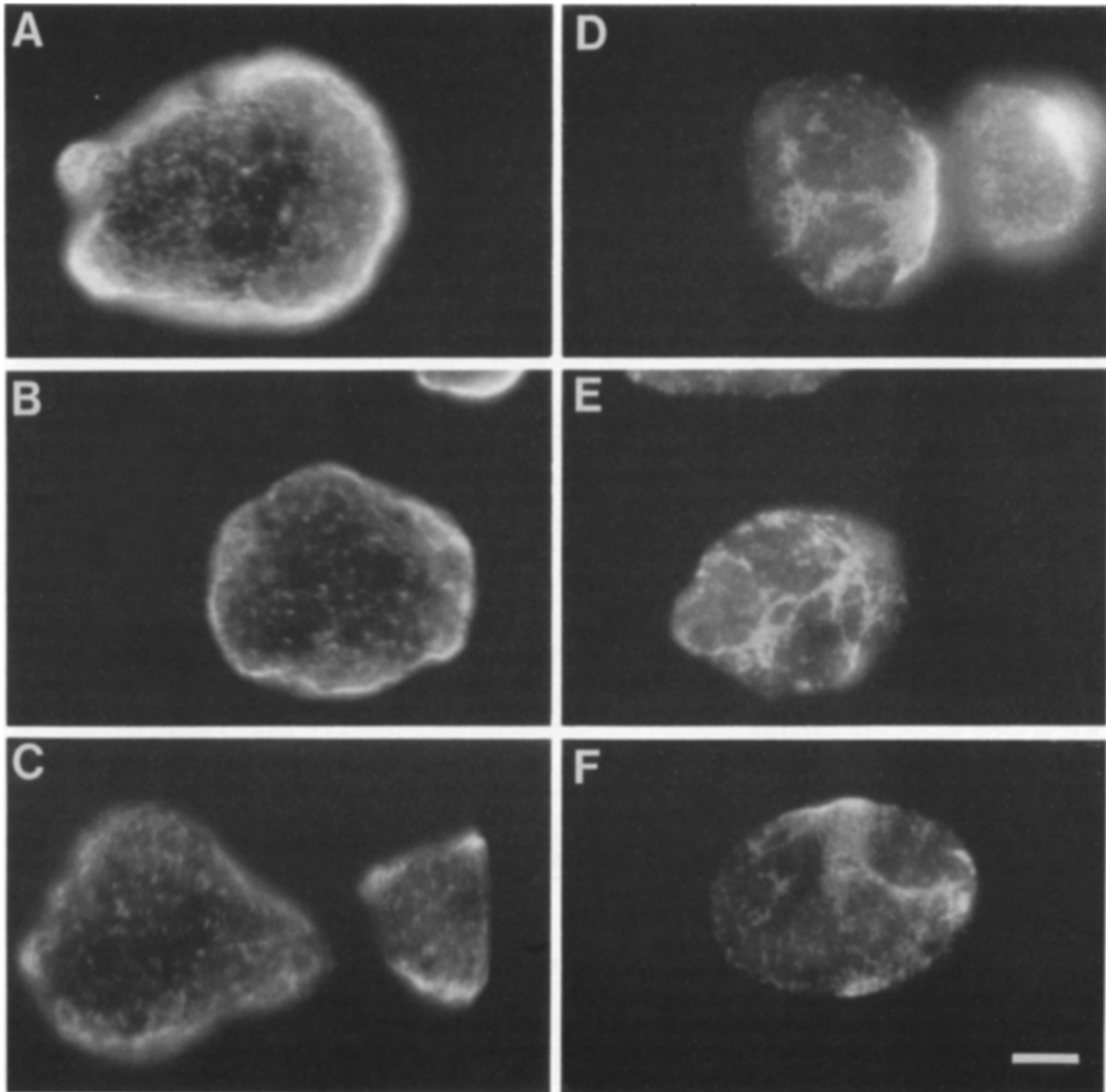
*Figure 8.* Immunolocalization of myosin. *A–C* show FITC antimyosin staining of HS2206 null cells transformed with pSB2, expressing full-length myosin. *D–F* show FITC antimyosin staining of HS2206 null cells transformed with pSB3, expressing the ΔC34-truncated myosin.

response to treatment with con A. When full-length and truncated myosin transformants were treated with rhodamine-labeled con A (TRITC-con A), both cell types formed discrete polar aggregations of con A with similar kinetics (Fig. 9). The intensity and uniformity of capping by full-length myosin transformants (Fig. 9, *middle row*) was indistinguishable from wild type Ax2 cells (not shown). The degree of capping induced in the truncated myosin transformants (Fig. 9, *bottom row*) was similar to that of full-length myosin transformants. Myosin null cells showed no capping response at all (Fig. 9, *top row*); at later time points patching became apparent on the null cells, and more brightly staining areas were seen that represent endocytosed material accumulating within the cells (apparent by focusing through the fixed cells).

It has been shown previously that myosin colocalizes with cap structures as they are forming in *Dictyostelium*, but that the myosin delocalizes from beneath the cap once the cap has formed (Carboni and Condeelis, 1985). These steps are then followed by gradual endocytosis of the capped surface proteins. We used this process as an assay to examine the recruitment and delocalization competence of the ΔC34-truncated myosin. Cells were treated briefly with con A, allowed to cap for either 4 or 30 min, and then fixed. These cells were then fluorescently stained for myosin. Full-length myosin transformants displayed a high frequency of myosin colocalization with caps when fixed at 4 min (Fig. 10, *A–C*), and almost never displayed myosin colocalized with the caps when fixed at 30 min (Fig. 10, *D–F*), consistent with the previously published behavior of wild type *Dictyostelium*
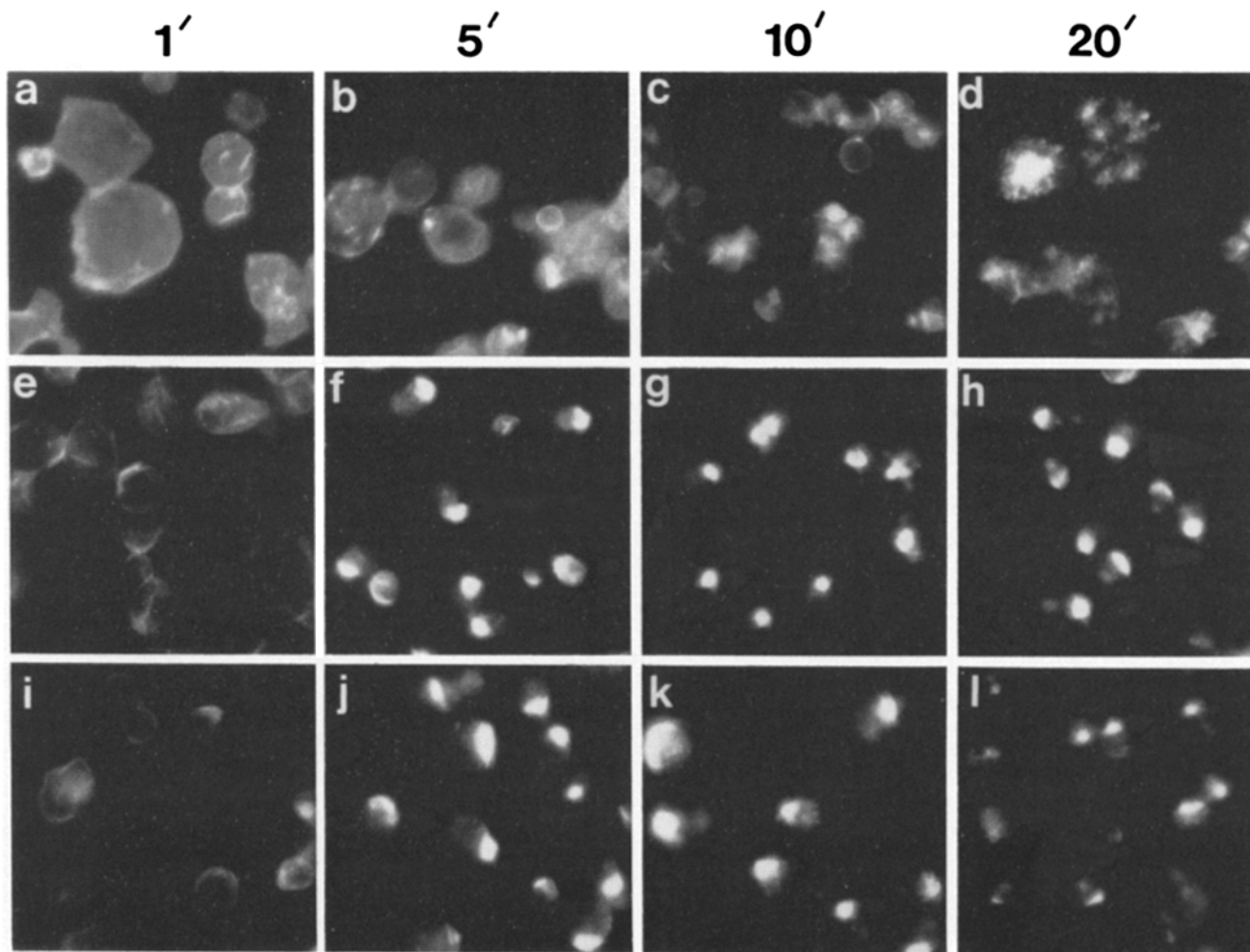
*Figure 9.* Con A-induced capping in transformants. Cells were attached to glass coverslips, treated with 30 µg/ml rhodamine-conjugated con A (TRITC-con A), and fixed at 1, 5, 10, and 20 min, as indicated at the top of the figure. (*a–d*) HS2206 null cells; (*e–h*) pSB2 (full-length myosin) transformants of HS2206 null cells; (*i–l*) pSB3 (truncated myosin) transformants of HS2206 null cells.

(Carboni and Condeelis, 1985). When fixed at 4 min, the ΔC34-truncated myosin transformants also displayed a high frequency of colocalization with caps (Fig. 10, *G–I*). In contrast to the full-length myosin transformants, however, these cells continued to display high frequencies of myosin colocalization with the caps at 30 min (Fig. 10, *J–L*), as well as at 60 min (data not shown). Although the truncated myosin at 30 min colocalized with high frequency, it consistently had a less compact appearance than at 4 min, with the periphery of the patch of myosin usually extending beyond the edges of the surface protein cap. This point is apparent by comparing Fig. 10, *H* and *I* to Fig. 10, *K* and *L*.

The frequency of myosin colocalization was scored for >200 cells for each of the time points above (Fig. 11). At the 4-min time point, both full-length and truncated myosin displayed high frequencies of colocalization with caps (72 and 99%, respectively). The colocalization of the truncated myosin was consistently more frequent and more intense than that of full-length myosin at this time point. At 30 min 95% of the truncated myosin transformants showed myosin colocalized with the con A caps, while only 4% of the full-length myosin transformants showed detectable colocalization. Endocytosis of the capped surface proteins did not appear to be severely impaired in the truncated myosin transformants; at 30 min both cell types showed roughly similar amounts of fluorescent cytoplasmic vesicles resulting from endocytosis.

## Discussion

The results reported here demonstrate that the carboxy-ter-

*Figure 10.* Association of myosin with con A-induced caps. Cells were attached to coverslips and induced to form surface protein caps with TRITC-con A as described under Materials and Methods. These cells were then fixed at 4 or 30 min after con A exposure and processed for immunofluorescent myosin staining, using an antimyosin antiserum and FITC-labeled secondary antibody. The left column shows phase-contrast images, the center column shows TRITC-labeled con A caps, and the right column shows FITC-antimyosin staining. *A–C* show full-length myosin transformants at 4 min; *D–F* show full-length myosin transformants at 30 min; *G–I* show ΔC34-truncated myosin transformants at 4 min; *J–L* show ΔC34-truncated myosin transformants at 30 min. Bar, 10 µm.
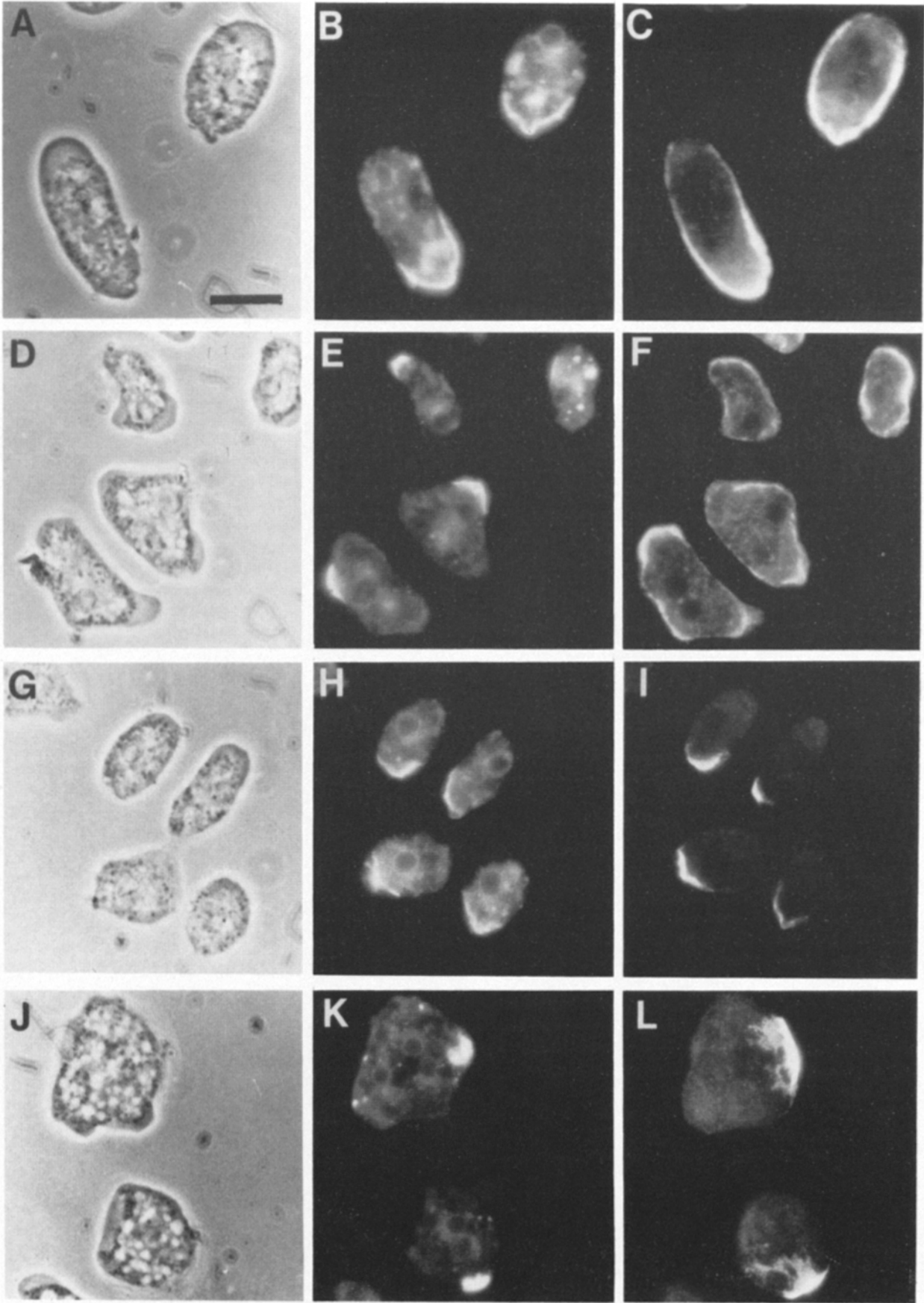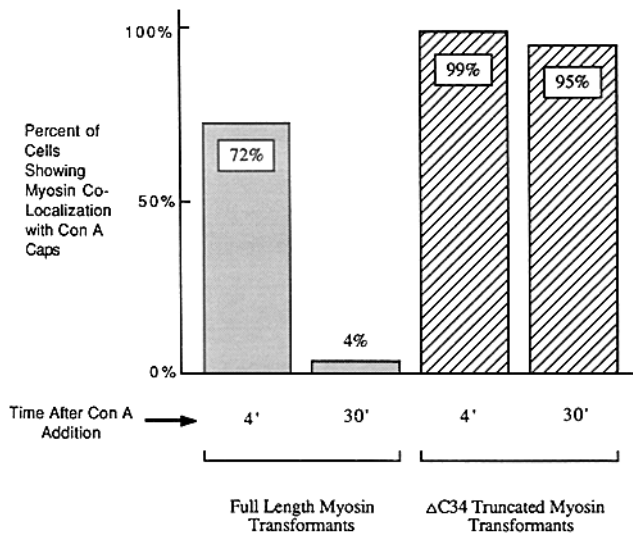
*Figure 11.* Quantitation of myosin colocalization with caps in full-length and ΔC34-truncated myosin transformants. Cells were treated as for Fig. 10 and scored for whether myosin showed distinct enrichment in the cortex of the cell underlying the cap structure. Greater than 200 cells were scored at each time point. Cells were scored as showing colocalization of myosin with the cap if the most intense area of myosin staining coincided with the location of the cap; in many cases a gradient of myosin staining intensity was observed (especially with full-length myosin at the 4-min point). Cells were chosen for scoring while observing the TRITC fluorescence channel (to monitor TRITC-con A), so that only cells that displayed capped surface protein were selected. For both cell types at the 30-min time point ~25–50% of the cells no longer had a clear single cap of fluorescent con A, and these cells were not included in the cell scoring.

minal 34-kD of the *Dictyostelium* myosin tail plays a key role in allowing the cell to disassemble myosin from contractile structures. The in vivo properties of the ΔC34-truncated myosin provide support for earlier studies with purified myosin that have implicated the carboxy terminus in control of assembly (Pagh et al., 1984; Kuczmarski et al., 1987; Ravid and Spudich, 1989; Vaillancourt et al., 1988). Based on those biochemical studies, we predicted that a ΔC34-truncated myosin would be relatively normal for recruitment to contractile structures and for contraction itself, but that disassembly of this protein from contractile structures would be impaired. Our results bear out this interpretation.

The strongest evidence that this domain is required for disassembly comes from the capping experiments. The kinetics of cap formation in the ΔC34-truncated myosin transformants is indistinguishable from the wild type or full-length myosin transformants, and the kinetics of colocalization of the truncated protein to the cap are similar as well. Unlike the full-length myosin, however, the truncated myosin remained highly colocalized with the caps for up to 60 min after initiation of capping. It is interesting that even at the 4-min time point, the truncated myosin consistently showed stronger colocalization with the forming cap of surface proteins. This result is consistent with a capping model in which myosin is responsible for sweeping patched surface proteins into the forming cap, and that once at the cap, myosin normally disassembles and cycles back into the cytoplasm. In

the truncated myosin transformants an apparent defect in the disassembly step results in excessive colocalization of the truncated myosin even at the early stages of the process. The less compact appearance of the colocalized truncated myosin at 30 min may reflect a relaxation that occurs after capping is complete and the contractile activity of the myosin is turned off (Bourguignon and Bourguignon, 1984).

Our working model for how the cell controls myosin relocalization is based on the idea that in a resting state the majority of the cellular myosin is monomeric and located in the cytoplasm. Upon stimulus for a contractile event, dephosphorylation of the heavy chains of these monomers leads to filament formation, concurrent with light chain phosphorylation that activates the contractile activity of the myosin. Myosin filaments would associate with the cortical cytoskeleton due in part to the increased affinity of the filaments relative to monomers for actin; recruitment to the cortex might also be stimulated by light chain phosphorylation or effects of other components of the cytoskeleton. Cortical filaments are presumed to be the active contractile form used by the cell; recruitment of filaments to specific regions of the cortex may occur by "cortical sliding," as discussed below, but other mechanisms that directly limit assembly to certain zones (e.g., the contractile ring in the furrow region) are not ruled out. Upon termination of a contractile event, myosin heavy chain phosphorylation and light chain dephosphorylation would occur, disassembling the cortical filaments, inactivating the actin-activated ATPase and contractile activity, and allowing monomers to redistribute to the cytoplasm. One implication of this model is that rapid dephosphorylation of cytoplasmic myosin must occur in response to recruitment signals; very little is known in regard to this point. The other components of the model are all consistent with current information regarding the biochemical properties of myosin and the in vivo properties presented in this work. In this model, the equilibrium between monomers and filaments would be shifted greatly towards filaments for the ΔC34-truncated myosin; this shift could be sufficient to confer cortical localization due to increased actin affinity, even in the absence of light chain phosphorylation. Because the ΔC34-truncated myosin heavy chains are not phosphorylatable at the end of a contractile event, the protein remains assembled in the cortex of the cell; the relaxation or spreading out of this material that is apparent after completion of capping (Fig. 10 *L*) may reflect the gradual diffusion of these filaments into the rest of the cortex once contraction is terminated. Clearly much work remains to be done to determine whether this model is correct and sufficient to explain myosin localization control.

Impaired disassembly of the cortical myosin in the ΔC34-truncated myosin cells might also explain their stiff appearance and lack of normal pseudopod dynamics. If pseudopod extension requires localized disassembly and rearrangement of the cortical cytoskeleton at a specific site, then the truncated myosin assembled into the cortex at such a spot would probably not disassemble properly, and might inhibit other events that would normally drive pseudopod extension.

The behavior of the truncated myosin transformants during capping also offers a possible explanation for the cortical patches of assembled myosin that were observed in cells that were not treated with con A. It is conceivable that the cortical aggregates of myosin filaments seen in the truncated myo-

sin transformants are remnants of contractile rings from previous division attempts. The myosin in these cells may be capable of correct recruitment to the contractile ring during cell division, but subsequently unable to disassemble. Steric hindrance of furrowing by this myosin that is impaired for disassembly might explain the aberrant divisions observed by video microscopy, as well as the slightly slower growth rate of these cells in suspension culture. We cannot exclude the possibility that these defects are the result of the reduced expression level of the truncated myosin (42% relative to myosin expression in wild type cells).

The fact that the ΔC34-truncated myosin transformants do seem to initiate cytokinesis suggests that the truncated myosin in these cells may be recruited to the forming cleavage furrow by cortical sliding rather than by disassembly and subsequent reassembly from the endoplasm. Recruitment of this myosin to the cleavage furrow via cortical sliding would support recently proposed models for contractile ring assembly (Bray and White, 1988), and would be consistent with the recent demonstration that F-actin can be recruited to the cleavage furrow without disassembly into monomers (Cao and Wang, 1990).

Cote and McCrea (1987) have performed biochemical analysis on a truncated *Dictyostelium* myosin very similar to the molecule that we have analyzed in vivo in this study. They used chymotryptic cleavage to remove a carboxy-terminal fragment of 33,700 D from the tail of the molecule, and demonstrated that the cleavage site was just after the tyrosine at position 1,825 of myosin. This site is only six amino acids past the position of the truncation we report here, so that one might expect these two myosins to have similar properties. The salt dependence of assembly of their chymotryptic myosin was generally similar to wild type unphosphorylated myosin, consistent with the idea that the domain that drives assembly lies amino-terminal to the truncation ("N34"; see Fig. 1), and consistent with the data presented here which indicates that the ΔC34-truncated myosin assembles in vivo. In preliminary biochemical studies, we find that purified ΔC34-truncated myosin also has a salt dependence of assembly that is similar to wild type unphosphorylated myosin (data not shown). One particularly interesting result from the Cote and McCrea work was that their chymotryptic myosin displayed only 20% of the wild type actin-activated ATPase. It will be of interest to determine whether the in vitro actin-activated ATPase of our ΔC34-truncated myosin is also reduced; the competence of ΔC34-truncated myosin for in vivo contractile processes would imply that the in vivo actin-activated ATPase of this molecule should not be substantially impaired. Such a discrepancy between in vivo and in vitro properties could conceivably reflect differences in structure between filaments formed in vivo and filaments formed in vitro.

O'Halloran and Spudich (1990) recently used a different method, based on homologous recombination, to generate a *Dictyostelium* cell line that produced a similar truncated myosin protein. Although their study did not address the cellular dynamics of the altered myosin, the resultant cell line, unlike the ΔC34-truncated transformants of our study, was unable to grow in suspension. We have determined that the expression level of the truncated protein in their cell line is 13% of wild type (SD = 3.7; $n = 6$), using the same quantitation method presented above for our cell lines. The low ex-

pression level in their cells probably accounts for the block they observed in cell division.

The results presented here demonstrate that the carboxy-terminal domain of *Dictyostelium* myosin plays a critical role in the regulation of myosin assembly into the cytoskeleton, and suggest that this domain may specifically mediate disassembly of myosin from the cytoskeleton after completion of a contractile event. Further analysis with other truncated myosin genes and with site-directed alterations of the myosin gene will allow precise identification of the critical residues in this domain. With these approaches it will be possible to determine whether it is the phosphorylation sites previously identified in vitro or other sequences within this domain that regulate the assembly state of the myosin molecule.

*References*

Berlot, C., J. Spudich, and P. Devreotes. 1985. Chemoattractant-elicited increases in myosin phosphorylation in *Dictyostelium. Cell.* 43:307–314.

Berlot, C. H., P. N. Devreotes, and J. A. Spudich. 1987. Chemoattractant-elicited increases in *Dictyostelium* myosin phosphorylation are due to changes in myosin localization and increases in kinase activity. *J. Biol. Chem.* 262:3918–3926.

Bourguignon, L., and G. Bourguignon. 1984. Capping and the cytoskeleton. *Int. Rev. Cytol.* 87:195–224.

Bray, D., and J. White. 1988. Cortical flow in animal cells. *Science (Wash. DC).* 239:883–888.

Cao, L., and Y. Wang. 1990. Mechanism of the formation of contractile ring in dividing cultured animal cells. I. Recruitment of preexisting actin filaments into the cleavage furrow. *J. Cell Biol.* 110:1089–1095.

Carboni, J., and J. Condeelis. 1985. Ligand-induced changes in the localization of actin, myosin, 95K (α-actinin), and 120K protein in amebae of *Dictyostelium discoideum. J. Cell Biol.* 100:1884–1893.

Collins, J., J. Kuznicki, B. Bowers, and E. Korn. 1982. Comparison of the actin binding and filament formation properties of phosphorylated and dephosphorylated *Acanthamoeba* myosin II. *Biochemistry.* 21:6910–6915.

Cote, G., and S. McCrea. 1987. Selective removal of the carboxyl-terminal tail end of the Dictyostelium myosin II heavy chain by chymotrypsin. *J. Biol. Chem.* 262:13033–13038.

De Lozanne, A., and J. Spudich. 1987. Disruption of the *Dictyostelium* myosin heavy chain gene by homologous recombination. *Science (Wash. DC).* 236:1086–1091.

Demerec, M., E. Adelberg, A. Clark, and P. Hartman. 1966. A proposal for a uniform nomenclature in bacterial genetics. *Genetics.* 54:61–67.

Egelhoff, T., S. Brown, D. Manstein, and J. Spudich. 1989. Hygromycin resistance as a selectable marker in *Dictyostelium discoideum. Mol. Cell. Biol.* 9:1965–1968.

Egelhoff, T., D. Manstein, and J. Spudich. 1990. Complementation of myosin null mutants in *Dictyostelium discoideum* by direct functional selection. *Dev. Biol.* 137:359–367.

Fukui, Y., S. Yumura, and T. Yumura. 1987. Agar-overlay immunofluorescence: high-resolution studies of cytoskeletal components and their changes during chemotaxis. *Methods Cell Biol.* 28:347–356.

Fukui, Y., A. De Lozanne, and J. Spudich. 1990. Structure and function of the cytoskeleton of a *Dictyostelium* myosin-defective mutant. *J. Cell Biol.* 110: 367–378.

Harrington, W., and M. Rodgers. 1984. Myosin. *Annu. Rev. Biochem.* 53: 35–73.

Kitanishi-Yumura, T., and Y. Fukui. 1989. Actomyosin organization during cytokinesis: reversible translocation and differential redistribution in *Dictyostelium. Cell Motil. Cytoskeleton.* 12:78–89.

Knecht, D., and W. Loomis. 1987. Antisense RNA inactivation of myosin heavy chain gene expression in *Dictyostelium discoideum. Science (Wash. DC).* 236:1081–1086.

Kuczmarski, E., S. Tafuri, and L. Parysek. 1987. Effect of heavy chain phosphorylation on the polymerization and structure of *Dictyostelium* myosin filaments. *J. Cell Biol.* 105:2989-2997.

Laemmli, U. 1970. Cleavage of structural proteins during the assembly of the head of bacteriophage T4. *Nature (Lond.).* 227:680-685.

Luck-Vielmetter, D., M. Schleicher, B. Grabatin, J. Wippler, and G. Gerisch. 1990. Replacement of threonine residues by serine and alanine in a phosphorylatable heavy chain fragment of *Dictyostelium* myosin II. *FEBS (Fed. Eur. Biochem. Soc.) Lett.* 269:239-243.

Maniatis, T., E. Fritsch, and J. Sambrook. 1982. Molecular Cloning: A Laboratory Manual. Cold Spring Harbor Laboratory, Cold Spring Harbor, NY. 545 pp.

Manstein, D., M. Titus, A. De Lozanne, and J. Spudich. 1989. Gene replacement in *Dictyostelium*: generation of myosin null mutants. *EMBO (Eur. Mol. Biol. Organ.) J.* 8:923-932.

Nachmias, V., Y. Fukui, and J. Spudich. 1989. Chemoattractant-elicited translocation of myosin in motile *Dictyostelium. Cell Motil. Cytoskeleton* 13:158-169.

Ogihara, S., M. Ikebe, K. Takahashi, and Y. Tonomura. 1983. Requirement of phosphorylation of *Physarum* myosin heavy chain for thick filament formation, actin activation of $Mg^{2+}$-ATPase activity, and $Ca^{2+}$-inhibitory superprecipitation. *J. Biochem.* 93:205-223.

O'Halloran, T., and J. Spudich. 1990. A genetically engineered truncated myosin in *Dictyostelium*: the carboxy-terminal domain is not required for the developmental cycle. *Proc. Natl. Acad Sci. USA.* 87:8110-8114.

O'Halloran, T., S. Ravid, and J. Spudich. 1990. Expression of *Dictyostelium* myosin tail segments in *Escherichia coli*: domains required for assembly and phosphorylation. *J. Cell Biol.* 110:63-70.

Pagh, K., H. Maruta, M. Clavicz, and G. Gerisch. 1984. Localization of two phosphorylation sites adjacent to a region important for polymerization on the tail of *Dictyostelium* myosin. *EMBO (Eur. Mol. Biol. Organ.) J.* 3: 3271-3278.

Pasternak, C., J. Spudich, and E. Elson. 1989. Capping of surface receptors and concomitant cortical tension are generated by conventional myosin. *Nature (Lond.).* 341:549-551.

Peltz, G., J. Spudich, and P. Parham. 1985. Monoclonal antibodies against seven sites on the head and tail of *Dictyostelium* myosin. *J. Cell Biol.* 100:1016-1023.

Peterson, G. 1977. A simplification of the protein assay method of Lowry et al. which is more generally applicable. *Anal. Biochem.* 83:346-356.

Ravid, S., and J. Spudich. 1989. Myosin heavy chain kinase from developed *Dictyostelium* cells: purification and characterization. *J. Biol. Chem.* 264: 15144-15150.

Schreiner, G., K. Fujiwara, T. Pollard, and E. Unanue. 1977. Redistribution of myosin accompanying capping of surface Ig. *J. Exp. Med.* 145:1393-1398.

Spudich, A. 1987. Isolation of the actin cytoskeleton from amoeboid cells of *Dictyostelium. Methods Cell Biol.* 28:209-214.

Sussman, M. 1987. Cultivation and synchronous morphogenesis of *Dictyostelium* under controlled experimental conditions. *Methods Cell Biol.* 28: 9-30.

Towbin H., T. Staehlin, and J. Gordon. 1979. Electrophoretic transfer of proteins from polyacrylamide gels to nitrocellulose sheets: procedure and some applications. *Proc. Natl. Acad. Sci. USA.* 76:4350-4354.

Vaillancourt, J., C. Lyons, and G. Cote. 1988. Identification of two phosphorylated threonines in the tail region of *Dictyostelium* myosin II. *J. Biol. Chem.* 263:10082-10087.

Yumura, S., H. Mori, and Y. Fukui. 1984. Localization of actin and myosin for the study of ameboid movement in *Dictyostelium* using improved immunofluorescence. *J. Cell Biol.* 99:894-899.